ADVANCED ENERGY MATERIALS
www.advenergymat.de

Evaluating the Use of Critical Current Density Tests of Symmetric Lithium Transference Cells with Solid Electrolytes

Till Fuchs, Catherine G. Haslam, Felix H. Richter, Jeff Sakamoto, and Jürgen Janek**

Alkali metal filament penetration into solid electrolytes causes short circuit induced cell failure, commonly evaluated using the bidirectional critical current density (CCD) test with stepwise increases in current density in alternating directions across symmetric lithium cells. However, the CCD is neither intrinsic to the cell nor to the material but rather depends on various extrinsic factors, such as current profile, transferred charge, pressure, resting intervals, and interface chemistry. The purpose of this study is to disambiguate the interpretation of CCD analyses in the literature and propose alternative approaches to analyze the stability and kinetics of the alkali metal/solid electrolyte interface. Two types of failure modes of electrochemical cells with solid electrolytes are defined: 1) failure of the solid electrolyte by crack formation coupled with or followed by dendrite growth, and 2) failure of the alkali metal electrode by the formation of pores at the interface with the solid electrolyte followed by filament initiation that eventually leads to short-circuiting. Therefore, the study recommends that CCD tests specify the failure mode. It is demonstrated that unidirectional polarization enablesunambiguous differentiation between failure modes. The proposals for bi- and unidirectional testing presented here are expected to provide more reliable and consistent CCD values across the community.

1. Introduction

Solid-state batteries (SSBs) have gained much attention based on the promise to exceed the performance of the lithium-ion battery (LIB) technology that relies on liquid electrolyte and intercalation-type electrodes.[1–5] This is largely based on the assumption that solid electrolytes (SEs) enable the use of high-capacity alkali metal as the anode material,[6–9] which would effectively increase the cell specific energy and energy density. To fulfill these expectations, the application of the alkali metal anode must still overcome several challenges before commercialization. The reactivity of lithium metal with ambient atmosphere[10,11] and with nearly every SE[12–15] often leads to highly resistive and unstable interfaces. Furthermore, several issues arise during the operation of metal anodes in contact with an SE. If the stripping (discharge) current exceeds a certain threshold, lattice vacancies are injected into the metal at a faster rate than can be replenished by diffusion and creep. The resulting vacancy accumulation leads to pore formation and high lithium transfer resistance at the interface.[16] In addition, filaments grow when the current is reversed to plating (charging) as the current is now limited to the remaining contact area.[17]

To determine the resistance to short-circuiting by the formation of dendrites, testing of the critical current density (CCD) using symmetric cells is frequently used in literature.[18–25] In the typical, bidirectional CCD test, a cell is cycled using a symmetric staircase galvanostatic test until a sudden drop in voltage to zero indicates short-circuiting by one or multiple dendrites, electronically connecting the electrodes. The obtained CCD is then defined as the lowest current density at which short-circuiting by filament growth occurs. Generally, the underlying failure mechanism when the CCD is reached can be a variety of different effects based on the used cell design, such as metal plating on graphite anodes, dendrite formation in both solid and liquid electrolytes, cracking of SEs, or even void formation.

While the CCD test highlights the importance of interface stability and kinetics, it often is misinterpreted as an inherent cell or even SE property. This appears to be a misconception considering the large discrepancy of the CCD results between different studies of comparable cells using alkali metal electrodes. The following discussion focuses on lithium metal anodes (LMAs) in

T. Fuchs, F. H. Richter, J. Janek
Institute of Physical Chemistry
Justus-Liebig-University Giessen
Heinrich-Buff-Ring 17, D-35392 Giessen, Germany
E-mail: Till.Fuchs@pc.jlug.de; juergen.janek@pc.jlug.de
T. Fuchs, F. H. Richter, J. Janek
Center for Materials Research (ZfM)
Justus-Liebig-University Giessen
Heinrich-Buff-Ring 16, D-35392 Giessen, Germany
C. G. Haslam, J. Sakamoto
Department of Materials Science and Engineering
University of Michigan
Ann Arbor, MI 48109, USA
C. G. Haslam, J. Sakamoto
Department of Mechanical Engineering
University of Michigan
Ann Arbor, MI 48109, USA

The ORCID identification number(s) for the author(s) of this article can be found under https://doi.org/10.1002/aenm.202302383

DOI: 10.1002/aenm.202302383

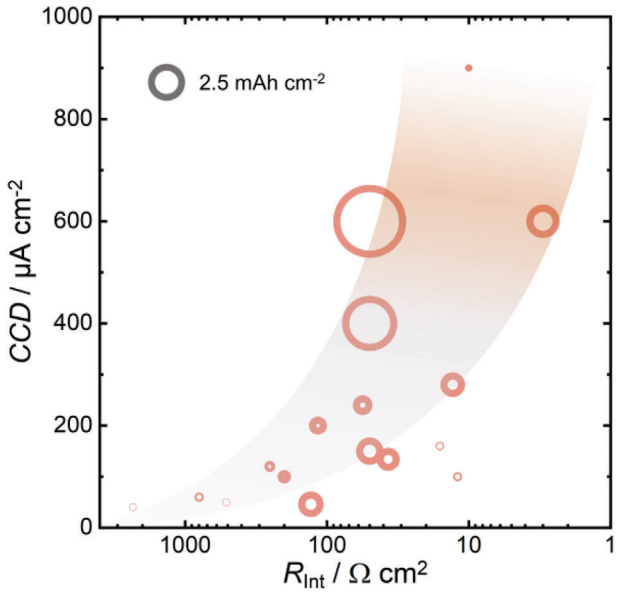

Figure 1. CCD results are taken from various reports on Li|LLZO|Li symmetric cells plotted versus the interfacial resistance. The area of the circles represents the cumulative charge that was cycled until a short circuit occurred. Despite the use of different dopants for stabilizing the cubic-LLZO, the widespread between the obtained CCD results is significant. This plot is based on a summary published by Flatscher et al. and excludes microelectrode measurements as well as 3D interfaces.[28] Cumulative charge values were extracted from the respective original publications.

combination with garnet-type LLZO as a model system, as this is one of the most widely studied LMA|SE combinations.

Figure 1 shows CCD results obtained for Li|LLZO|Li symmetric cells with planar interfaces, that were reported in different studies and with different testing conditions. The values are plotted versus the interfacial resistance as this appears to be the most influential parameter on the obtained CCD. A large spread of CCD values from 0.03 to 1 mA cm^{-2} has been reported for Li|LLZO|Li. This comparison does not include porous interfaces or microelectrode measurements,[23,26,27] which are difficult to compare owing to the strong difference in cell integration and testing conditions.

The CCD is very sensitive to external factors and variables, such as small defects from cell preparation or the used cycling protocol. Additionally, interpretation is further complicated due to overlapping microscopic effects and the difficulty to exclusively link dendrite nucleation or pore formation to one of the electrodes, especially when they overlap as shown by Kasemchainan et al.[29] Generally, cell failure can be due to failure of the SE itself, e.g. by lithium penetration and coupled crack formation or it can be induced by a failure of the LMA|SE interface, e.g., due to contact loss. In the first case, the LMA|SE interface is still in a low-resistance, conformal state but dendrites penetrate the SE coupled with cracking, which is a limitation imposed by the SE itself. In the latter case, however, pores form during anodic dissolution and then facilitate the growth of dendrites due to the current focusing at the remaining contact spots.[17,30,31] This is not an inherent limitation imposed by the SE but rather the LMA|SE interface. Therefore, it needs to be decided whether the SE itself or rather the electrode|SE interface is subject to investigation, and suitable test parameters need to be chosen before CCD measurements are conducted.

In our opinion, the dependence of the CCD and the underlying failure mechanisms on the testing parameters is fundamental, and an intentionally designed testing protocol is required to ensure the comparability of results between different studies. To derive guidelines on how to systematically determine the CCD on a given system, the relevant variables are discussed here first.

1.1. Applied Current-Time Profile (Transferred Charge)

CCD tests usually start with the application of a low current initially, followed by a stepwise current increase until short-circuiting of the cell. The cell voltage is recorded throughout the measurement. One very important factor that influences the outcome of the test is the duration of the galvanostatic step, i.e., the transferred charge. If only a low amount of charge is transferred per current step, a relatively high CCD is expected simply because the amount of lithium plated per step is insufficient to grow a long lithium filament and cause a short circuit, especially in the case of mm-thick laboratory samples. This phenomenon is sometimes referred to as "dynamic short-circuiting",[32] implying that a CCD threshold is exceeded without the typical hard drop to zero in cell voltage as dendrites are dissolved again upon current reversal. Therefore, shuttling a large amount of charge therefore results in a more relevant CCD value, having practical charge-discharge cycles in mind.

However, if a large amount of charge is shuttled during every step, pore formation occurs at the electrode during the stripping process, which leads to rapid short circuit upon current reversal. If the dendrite susceptibility of the SE is the property of interest, the actual CCD is thus underestimated. The significance of the charge transferred during a CCD test to yield a reasonable value was already recognized and investigated by Lewis et al. and expected to be 2.4 mAh cm^{-2} at minimum for their Li|Li_6PS_5Cl|Li cells.[33] Additionally, Reisecker et al. carried out further analysis showing how advanced cycling protocols including µs-pulsing affect the CCD results by limiting the time for a lithium activity build-up required for the formation of dendrites.[34] Finally, the current step height is also of relevance. Large step increases in applied current lead to an overestimation of the CCD because the true value may have been surpassed within the step. In any case, the specific current-time profile, together with the geometry of the electrode arrangements must be documented.

Unfortunately, it is also possible that a very high electronic current density (>10 mA cm^{-2}) passes through the cell unknowingly through a lithium filament in a shorted cell, yielding extremely high but incorrect values of the CCD. This may occur through erroneous pre-conditioning (e.g., combined pressure/heating step), which may lead to a lithium filament short-circuiting the cell already before the CCD test is started. This must be checked initially by careful impedance analysis and evaluation of the cell voltage during the test.

1.2. Applied Pressure and Waiting Time

One severely underestimated and also underreported factor influencing the CCD is a pause before current reversal. This pause

can be introduced either deliberately as a waiting step, but also unintentionally by acquiring an impedance spectrum over several minutes. If no pressure is applied during the measurement, this waiting step is expected to be less influential. However, if pressure is applied during the test, this waiting step changes the interface morphology due to creep or plastic deformation within the LMA.[35,36] For example, if pores have formed at the interface during the prior current step, they would have time to close and the interface morphology would return to its pristine state within a given waiting time before the next current step is applied. If probing the SE is of interest, this may be desired. However, if the LMA|SE interface is probed with the addition of long waiting times, the CCD is severely overestimated, especially if considerable stack pressures are applied. However, recent works show that too high pressures may even lead to detrimental effects, such as fracture of the SE,[37] excessive lithium creep through the SE at long waiting periods[38] and even crack/dendrite deflection based on stress applied orthogonal to the current direction.[39] These works overall showcase the strong and complicated influence of the cell stack pressure on the CCD.

1.3. Interface Conditions

The initial morphology and interface resistance are of utmost importance and influence the CCD test drastically.[20] As the interfacial resistance of pristine Li|LLZO interfaces is mainly governed by constriction resistances, high initial interface impedance results from a low contact area. This can either be caused by resistive passivation layers such as Li_2CO_3 on LLZO or from imperfect lithium preparation and integration.[10] Optimization of the interface is also the reason why the reported CCD for LLZO improved progressively over the years. For example, in 2011 a CCD of <0.025 mA cm^{-2} was obtained with an initial R_{int} > 5000 Ω cm^2.[40] Despite no changes of the bulk SE, this value quickly improved to 0.15 mA cm^{-2} at an R_{int} < 50 Ω cm^2 in 2015,[41] followed by >0.3 mA cm^{-2} at R_{int} < 5 Ω cm^2 in 2017.[20] For optimized interfaces with negligible interfacial resistance, a CCD of 1.0 mA cm^{-2} was reported in 2018.[42] However, measurements with single-crystalline LLZO and varying interfacial resistance imply that the CCD of Li|LLZO would only be ≈ 0.28 mA cm^{-2} at best,[28] which is well below practical targets.[43,44] Clearly, these results undeniably show that the CCD is not an inherent property of the SE but rather is strongly influenced by testing conditions and interface engineering.

1.4. Electrode and Pellet Geometry

Once different cell and electrode geometries are used, which are rarely reported, CCD results cannot reasonably be compared anymore. For example, a thicker pellet or SE sheet for testing the CCD has a higher resistance to filament penetration. In the case of dynamic short-circuiting, i.e., filament growth and dissolution without reaching the other electrode,[32] a thicker pellet is able to withstand higher current densities simply due to the fact that a dendrite has a further distance to penetrate. Furthermore, mm-thick pellet type SEs in a laboratory are able to homogenize the electric field across the cell, if constriction occurs at one of the respective electrodes.[45,46] If current constriction occurs at a porous electrode during stripping at a thin separator (e.g., 40 µm), the electric field distortion can reach the counter electrode, thereby influencing its plating performance, too.

Not only does the SE thickness have a profound influence on the CCD, but the electrode area and shape also influence filament initiation and propagation. For example, the likelihood of an electrode covering surface defects such as pits and scratches on a SE pellet surface increases with increasing electrode area. Since such defects facilitate the growth of lithium dendrites, using larger electrodes may lead to lower CCD values despite using the same SE or interface preparation method. This is supported by microelectrode measurements that show comparatively high CCDs of several tens of mA cm^{-2} (at very small contact areas in the order 10^{-4} cm^2).[26]

1.5. Influence of Temperature

The temperature influences the CCD by enhancing both the SE ionic conductivity as well as the vacancy diffusion within the lithium metal, which induce complex changes to the outcome of the CCD test. Most importantly, lithium metal gets more ductile at elevated temperatures. When 5 MPa of stack pressure is applied at moderate 35 °C to 50 °C, it already facilitates the collapse of pores induced by inhomogeneous stripping with 0.3 mA cm^{-2} and increases the CCD as discussed recently by Zaman et al.[47] Furthermore, temperatures above the melting point of lithium can help to negate the issue of pore formation completely, since vacancy diffusion in molten lithium is orders of magnitude faster than in the solid.[48] A general trend for higher CCD values is expected with increasing temperature and even small temperature differences in the order of 10 K may cause significant changes. Therefore, to better compare CCD values, the test temperature should be specified. Specifically, room temperatures can vary from lab to lab. Thus, if possible, the cell temperature should be reported as a specific value instead of "room temperature".

1.6. Impact of Lithium Metal Properties

The properties of the metal electrode itself in symmetric Li|SE|Li cells are frequently overlooked, in part due to the difficulty of characterization of LMAs. This includes chemical purity and microstructure, such as grain size and dislocation density although this is expected to strongly impact the electrode performance.[49] The biggest difference is expected when a lithium foil is compared to electrodeposited lithium in reservoir-free cell designs due to different microstructures and morphologies. However, since it is possible to deposit thick, homogeneous lithium films,[50,51] studying the influence between both types of lithium is certainly desired.

Additionally, commercial battery grade lithium foils usually contain up to 200 ppm of sodium amongst other impurities,[52] while electrodeposited lithium on a current collector is electrochemically purified by the ion selective properties of the SE. The impact of the purity of the LMA on the available discharge capacity is not quantified to date, but is expected to be

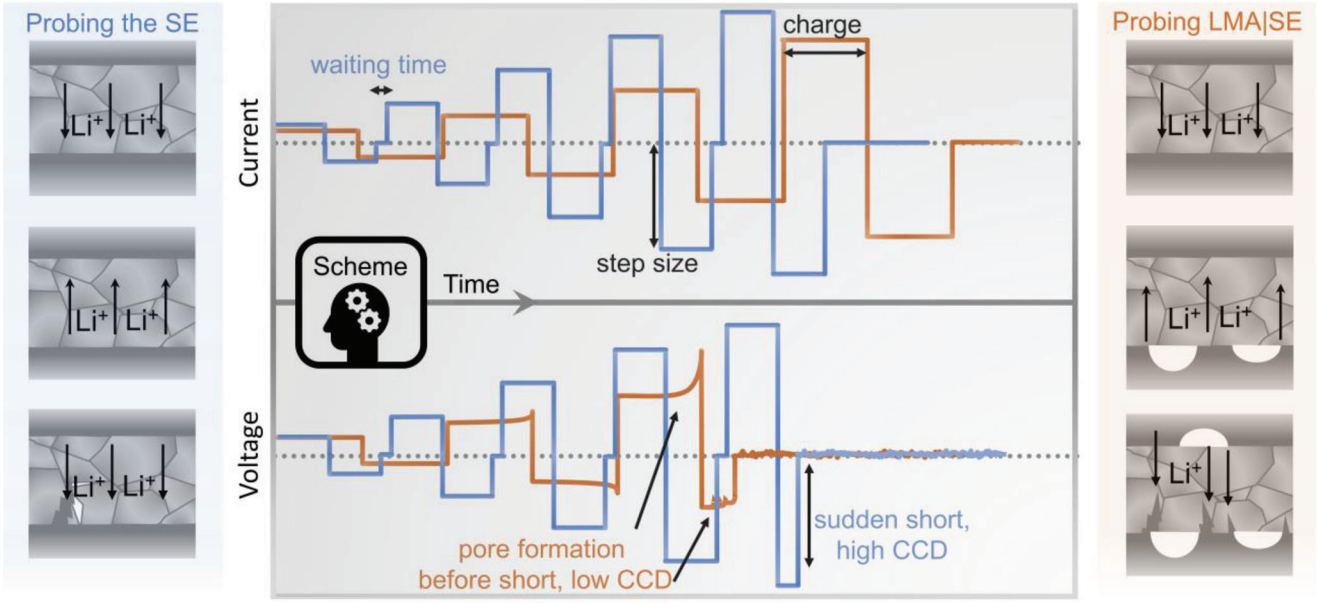

Figure 2. Idealized applied current profile (top) and schematic resulting voltage profile (bottom) to probe either the dendrite susceptibility of the SE (blue) or the LMA|SE interface (orange) using the example of a symmetric Li|SE|Li cell.

quite significant.[53] Similarly, the microstructure, grain size and dislocation density of the LMA also affects its electrochemical performance,[49,54] and is completely unknown to date for electrochemically deposited lithium. However, lithium deposited in situ may enable higher accessible stripping capacities than applied lithium foil,[51,55] albeit the comparison is difficult due to its different thickness.[56] It is unkown if the microstructure of lithium deposited on a lithium foil matches the initial microstructure of the lithium reservoir. Further, the deposition parameters such as current density and temperature also influence the microstructure of the deposited lithium. All these questions remain unanswered to date and may significantly change the output of a CCD test.

2. Results and Discussion

2.1. Guidelines on How to Separate direct SE Failure from Interface Failure

Within this chapter, guidelines are proposed to measure more meaningful CCD values for each failure mechanism using symmetric cells with LMAs. First, it needs to be decided whether the SE itself is to be primarily tested or whether the interface to the LMA lies in the focus of investigation. For example, if parameters only concerning the SE are changed within the study, such as grain size or chemical composition, it is reasonable to design a CCD test protocol to probe for direct separator failure. In contrast, when the study involves diverse interface modifications such as interlayers, it is important to characterize the LMA|SE interface using CCD test parameters that do not suppress interface issues. This could for example be relevant when high stack pressure is applied, as this can suppress interface related pore formation.[57] While designing a test that completely differentiates between the two cases is difficult, it still is useful to rationally test for either failure mechanism, thereby having more reliable test results.

The interface morphology evolution for the different failure cases is schematically depicted in **Figure 2**. For probing the SE, it is mandatory that pore formation at the LMA interface is avoided as such pores serve as a precursor for dendrite formation. Avoiding pore formation is possible by maintaining a stack pressure of a few MPa throughout the measurement and by introducing a resting time between the current steps. In general, the applied pressure helps to supply lithium via plastic deformation to the interface, avoid pore formation during stripping and remove residual pores during the resting time.[58,59] However, depending on the material system and geometry of the investigated cell, use of excessive stack pressures can fracture the SE and facilitate dendrite growth. In contrast, probing the LMA|SE interface works best without applying stack pressure and when a larger amount of charge is shuttled per current step. In this case, pores form above a certain current density, which then act as a precursor for filament formation because of current focusing at the remaining contact spots.

Figure 2 shows two idealized current profiles with which to test either the SE (blue) or the LMA|SE interface (orange) using the example of a Li|SE|Li cell. The respective resulting voltage profiles are also depicted schematically. The CCD value obtained for the blue test protocol is typically higher as stack pressure is applied to the cell during the measurement, which avoids pore formation. Moreover, a sudden voltage drop is observed for testing the SE as the resistance remains constant until a filament grows suddenly and short-circuits the cell. On the other hand, the orange protocol testing the LMA has a larger charge per step and there is no stack pressure applied to the cell. Here, voltage deviation occurs even before short-circuiting is complete: the voltage increases during a current step due to pore formation as described by Zhao et al.[60] and voltage

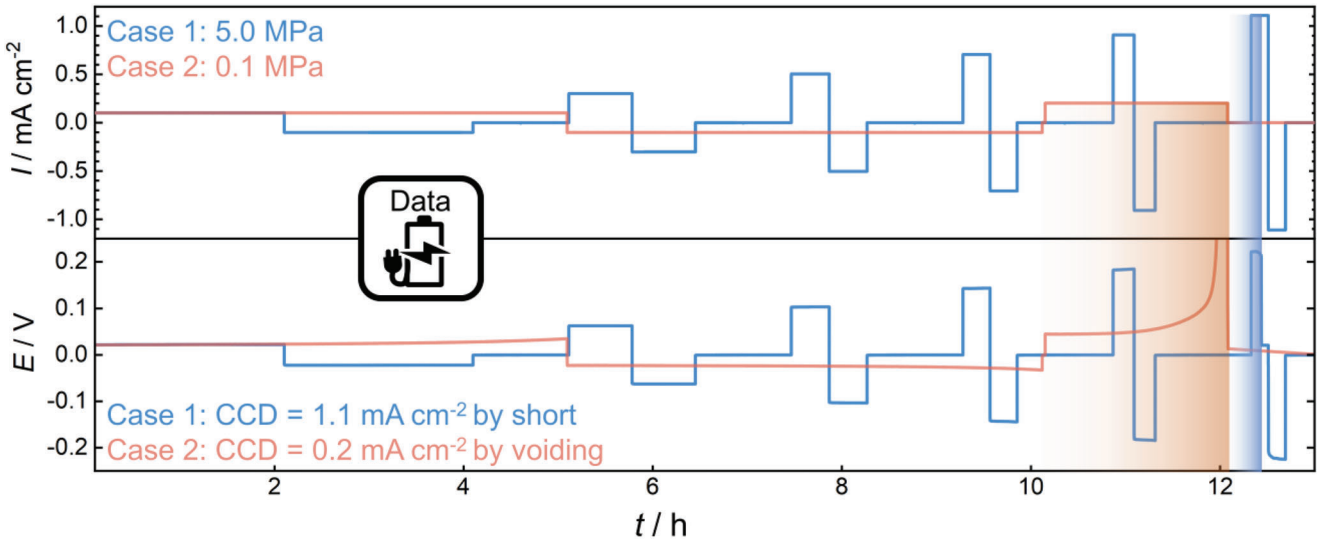

Figure 3. Measurement of the CCD of two Li|LLZO|Li cells at 25 °C following the examples specified in Figure 2 to showcase the drastically different failure mechanisms and obtained CCD values under different measurement conditions.

fluctuation occurs due to spallations and dendrite growth as analyzed by Ning et al.[58] Consequently, the CCD obtained with this test is substantially lower as a different failure mechanism occurs.

Measurements recorded in experiments that exemplify the cases defined in Figure 2 are depicted in **Figure 3**. In case 1, the electrolyte is investigated regarding its resistance to dendrite formation in a Li|LLZO|Li cell while applying 5.0 MPa of stack pressure, short current steps, and intermittent waiting steps. A CCD value of 1.1 mA cm^{-2} is obtained, as indicated by a sharp and sudden drop in cell voltage, with only minor changes to the cell voltage during previous steps. On the other hand, the electrode in a similar Li|LLZO|Li cell was investigated in case 2 by applying very small stack pressures of 0.1 MPa and long (dis)charging steps without additional resting time. Simply by changing the measurement parameters, the apparent CCD value drops to 0.2 mA cm^{-2} in this example. As predicted in the schematic of Figure 2, this cell does not fail because of a dendrite short-circuiting the cell, but due to high polarization induced by pore formation, which is evident from the strong increase in

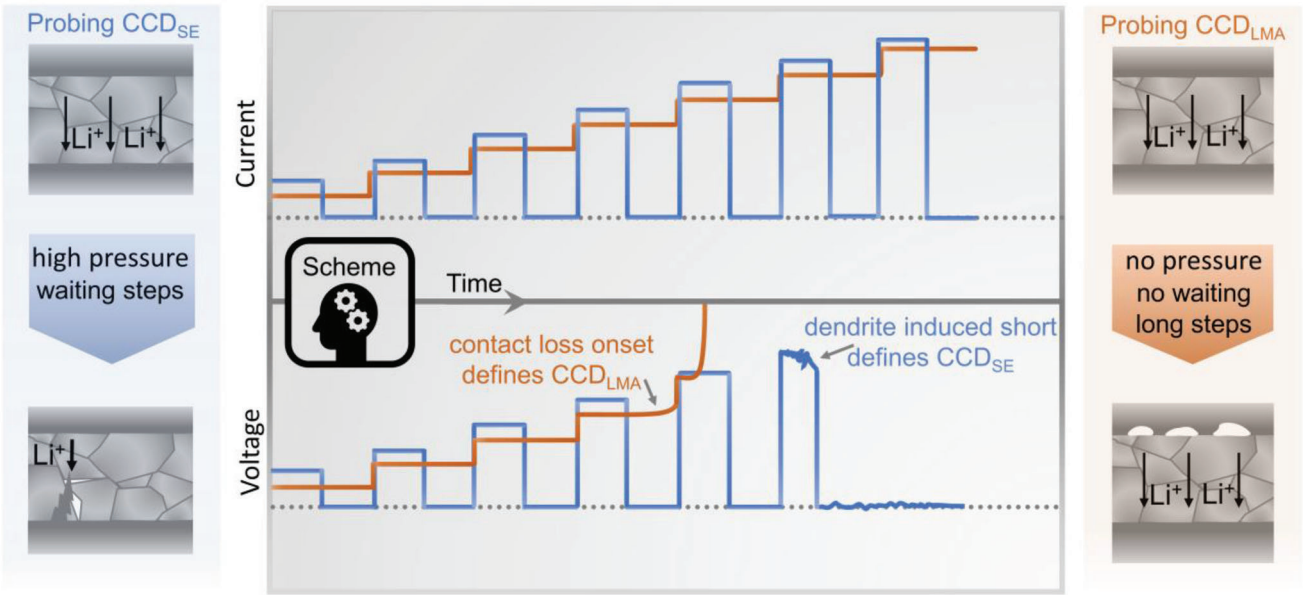

Figure 4. Idealized schematic showing a proposal for unidirectional testing of the CCD_{SE} (blue) or CCD_{LMA} (orange) in the top. The bottom part shows typical and desired voltage responses to the testing parameters and current applied. Furthermore, the graphics at the sides show the respective failure mechanisms for the CCD_{SE} (dendrites) and CCD_{LMA} (pore formation) and parameters on how to influence that mechanism likely occurs.

overvoltage. Furthermore, this polarization was already hinted at in prior steps by small increase of the overvoltage.

2.2. Unidirectional Tests as a Means to Counter the Sensitive Nature of Cycling

Unfortunately, the differentiation made in the last chapter between probing the SE or the LMA interface is not as clear-cut as it seems. Especially at higher current densities, it is difficult to suppress pore formation even when stack pressure is applied while probing the SE. Furthermore, cycling symmetric cells over many steps amplifies small interfacial issues that may arise during preparation. For example, small pores present upon cell assembly or surface defects within the SE are negligible at the beginning. However, they act as nucleation points for morphological instabilities, be it either pores or dendrites, and grow to significantly influence subsequent steps.

Several strategies can be used to circumvent the sensitive nature of bidirectional CCD tests. One is to conduct a high number of tests and perform a statistical analysis of CCD results, which is time-consuming and not feasible under basic laboratory conditions. Another method was recently proposed by Klimpel et al. as a means to standardize CCD tests.[61] It is suggested to reduce the areal capacity per half cycle in steps from 0.1 mAh cm^{-2} down to 0.01 mAh cm^{-2}, thereby analyzing the current density at which a short circuit is observed and avoiding the influence of pore formation during stripping. However, their voltage profiles still show severe polarization at higher current densities with the signature of pore formation before shorting,[9,30] which means that despite the very low shuttled areal capacities, an unpredictable interplay of pore formation, current constriction and dendrite formation governs the CCD. Therefore, we suggest the execution of unidirectional tests, which offers several benefits when compared to bidirectional cycling tests.[32,53,62–64]

In unidirectional tests, the current direction is not alternating between the steps. This limits the overlap of different mechanisms occurring in a cell, since lithium is consistently deposited at one electrode and stripped at the other electrode, drastically limiting the interdependence of these different microscopic effects. Hence, contact loss or dendrite formation as indicated by voltage features within the test can be unequivocally linked to one of the respective electrodes. This can, in principle, also be achieved with the introduction of a reference electrode (RE) during cycling. However, depending on the used SE, this is not trivial and requires careful cell design to avoid an influence of the RE on the system itself.

Therefore, it is reasonable to define two different critical currents based on the respective failure mechanism.[29,65] If the LMA fails during stripping because of pore formation and contact loss, the critical current density for stripping (CCD_{LMA}) is exceeded. If, however, a short circuit occurs at the plating electrode, the critical current density for plating (CCD_{SE}) is exceeded. While both effects overlap in bidirectional cycling tests, unidirectional tests allow to differentiate both mechanisms.

Obviously, impedance contributions arising from plating and stripping cannot be completely decoupled in a symmetric cell without an RE. Consequently, testing parameters need to be chosen with care to induce a failure of the electrode of interest with the other electrode remaining basically unchanged. Several parameters can be adjusted to account for this, as is the case for bidirectional CCD tests. Applied pressure, temperature, step size and height as well as waiting time between steps influence unidirectional tests in a similar way.

To determine the CCD_{SE}, it is of utmost importance to suppress pore formation at the stripping electrode. Like in CCD tests, this can be done by resupplying lithium to the interface via plastic deformation and creep, both being enhanced by increasing the temperature and applied stack pressure. Waiting steps while holding the pressure also shift the test to rather characterize the SE in unidirectional tests, similar to the discussion above. However, the stripped electrode, despite not being of interest in a CCD_{SE} test, still needs to be able to offer sufficient lithium. Depending on the test parameters, lithium foils of >100 µm thickness may need to be employed as the counter electrode.

Figure 5 shows exemplarydata recorded in experiments to obtain the CCD_{SE} (case 3) and CCD_{LMA} (case 4) with unidirectional tests using Li|LLZO|Li cells. We find that in the blue curves, applying pressure and incorporating a waiting step leads to rather stable charging steps with minor changes in overpotential, which lead to a dendrite induced short circuit at 1.1 mA cm^{-2}. Due to quite similar test parameters, this value coincides with the value obtained from the CCD measurement in Figure 3. However, the major advantage using the unidirectional test is that the dendrite initiation can be linked exclusively to the plating electrode.

The orange curve represents the test protocol and resulting cell voltage to test the CCD_{LMA}, as a minimal pressure is applied, and long charging steps are used. In accordance with previous reports, a current of 0.1 mA cm^{-2} is sufficient to induce very high polarization due to pore formation, if a large amount of charge >1 mAh cm^{-2} is transferred per step. This is especially important, as the capacity targets set in literature[2,43] of >5 mAh cm^{-2} by far exceed what is typically used in CCD tests per step. This means that to date, no planar Li|SE configuration is able to provide enough charge to meet the area capacity requirement at ambient temperature even at very low current densities far below practical targets if no significant stack pressure is applied.

Choosing the right charge per step is even more critical than in bidirectional CCD tests when testing unidirectionally. A charge that is too low results in an overestimation of the CCD_{SE}/CCD_{LMA}, because the failure onset may already occur in one step but is progressing to noticeable cell failure only in the subsequent step. For example, the CCD_{LMA} may be exceeded during a stripping step, but not enough charge is passed for pore formation to be observed. The pore formation would then only be noticed in the subsequent step, leading to an overestimation of the CCD_{LMA}. For ideally reversible Li|LLZO interfaces, the amount of charge that results in voiding is ≈1 to 2 mAh cm^{-2}.[26,30,66] To avoid such an underestimation, it is reasonable to test each current density in one cell without the step-wise increase. Each cell is then stripped with a higher current density until its individual failure occurs. While time-consuming, this procedure prevents erroneous interpretation of CCD_{LMA} or CCD_{SE} results, especially as the CCD_{LMA} seems to be substantially lower than the CCD_{SE}.[26,29]

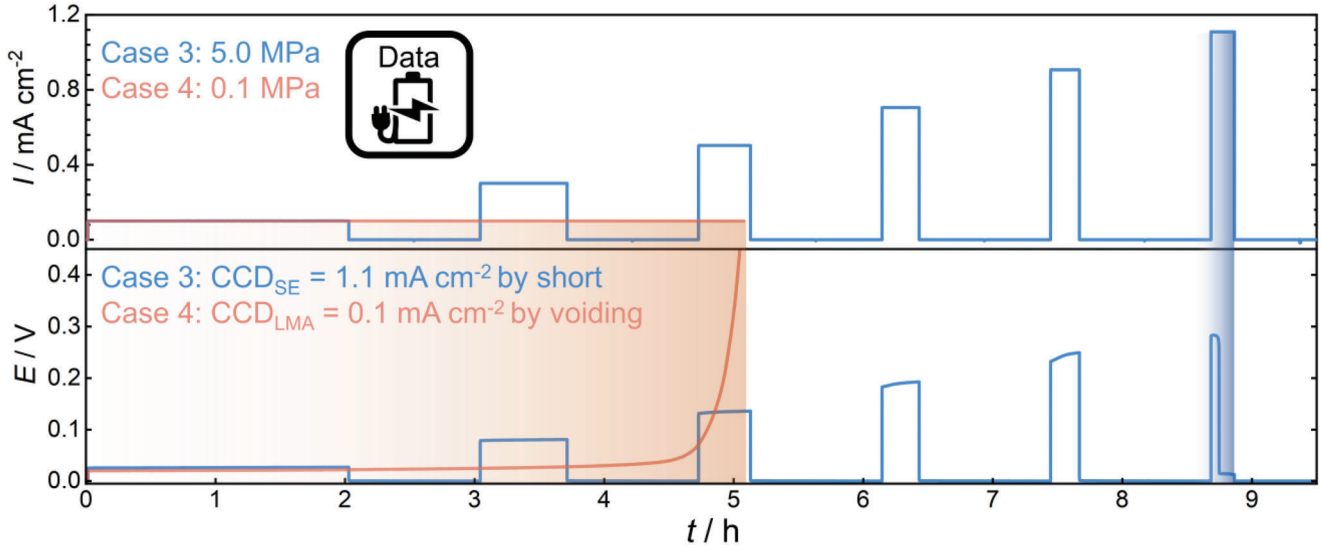

Figure 5. Measurement of the CCD_{SE} and CCD_{LMA} for two Li|LLZO|Li cells at 25 °C following the examples described in **Figure 4** to showcase the influence of the drastically different failure mechanisms also in unidirectional tests.

2.3. Comment on the Applicability of CCD Tests with Regards to Practical Cycling Profiles

While it is informative to assess the role that the electrodes or electrolytes play in controlling the rate capability, CCD tests do not sufficiently resemble the actual cycling profile of practical applications, e.g. typical use profiles of electric vehicles. For example, if an actual application requires the LMA to have a minimum area capacity of 5 mAh cm^{-2},[43] this corresponds to ≈30 µm of lithium or 50 h of stripping with 0.1 mA cm^{-2}. This is well above what is typically tested per step within CCD tests in literature. We therefore advocate to aim for higher test capacities, especially as some failure mechanisms like pore formation can only be noticed after a sufficient amount of lithium has been stripped.[30,63]

Furthermore, we can take the cycling profile of a traction battery used in an electric vehicle into account. Traction batteries usually have a highly asymmetric, discontinuous, and dynamic usage profile due to the varying user demands. For example, the current density during charging can be widely different and depends on whether the respective electric vehicle is charged over night at home with low current densities or at a charging stop when traveling with powers up to >270 kW at pack level or current densities of 12 mA cm^{-2} at cell level.[2,67] Discharge currents of such a cell also range from very slow rates when idling to several amperes when utilizing the maximum power the cell can provide. Additionally, both the charging and discharging processes are usually discontinuous and full of gaps, e.g., during short, daily commuting with the electric vehicle.

In consequence, CCD values or rather electrode specific rate limitations obtained in a well-defined laboratory test environment cannot guarantee that similar currents can be reached in an actual cell. Vice versa, it can be possible based on the specific cycling profile to obtain higher currents in real cells than what is predicted in CCD tests. With these considerations in mind, CCD tests should be carefully executed and reported on the one hand, and the results should not be overrated with respect to practical applications. CCD tests with typical laboratory cells have only limited relevance for large scale cells with completely different geometry and charge/discharge profiles.

3. Conclusions

The interpretation of CCD measurements and their widespread use in the study of metal electrodes is evaluated. Due to the large number of influential experimental and material parameters, CCD tests must be conducted very carefully, and the experimental conditions specified meticulously. Therefore, the results must always be considered in combination with the used cell design and test procedure.

Generally, two types of failure mechanisms can be specified in bidirectional CCD tests. One is due to a direct failure of the electrolyte itself, e.g., by fracture coupled with dendrite formation, and the other is due to pore formation in the metal preceding the short circuit, which facilitates the nucleation of dendrites. To steer the test to induce either failure mechanism, different parameters are recommended. In the case of testing for direct SE failure, interfacial pore formation should be suppressed by elevated stack pressure and temperature. For a full separation of dendrite and pore formation, we propose the use of unidirectional CCD tests to eliminate uncertainties present in bidirectional CCD tests. This leads to a separation of the CCD in a CCD_{SE} upon plating and a CCD_{LMA} upon stripping as showcased with Li|LLZO|Li cells herein. Our proposed external test parameters are generally also applicable to other metal electrodes, such as sodium or even magnesium.

Besides our guidelines on how to obtain reproducible and interpretable results, a variety of tests are still required to fully assess the rate capability of a given cell or electrode system. Especially regarding practical cell application, extensive testing should consist of a variety of different CCD_{SE} and CCD_{LMA} tests including very inhomogeneous and asymmetric cycling.

4. Experimental Section

Cell Preparation and Characterization: For CCD measurements of this work, LLZO:Ta ($Li_{6.5}La_3Ta_{0.5}Zr_{1.5}O_{12}$) was used, which was prepared as previously reported by Taylor et al.[42] Lithium electrodes were prepared according to Sharafi et al. and ≈700 µm thick, covered with thin nickel plates.[68] Electrochemical characterization was carried out using a VMP300 potentiostat by BioLogic in combination with the software EC-Lab (V. 11.36). Cell testing was carried out in an argon-filled glovebox (Vacuum Atmospheres Co.) with atmosphere < 1 ppm O_2 at a temperature of 25 °C. Pressure was applied during cell testing using a load frame (Imada, Inc.) with custom pressure clamp. The LLZO pellets used herein have a diameter of 12.7 mm, a thickness of ≈2 mm and circular electrodes with a diameter of 7.9 mm.

Acknowledgements

The authors want to thank Elisa Monte for her support with designing the ToC image and Till Ortmann for fruitful discussion. This work was conducted as part of the US-German joint collaboration on "Interfaces and Interphases in Rechargeable Li-metal based Batteries" supported by the US Department of Energy (DOE) and German Federal Ministry of Education and Research (BMBF). This work was partly funded by the German Federal Ministry of Education and Research (BMBF) under the project "LiSI 2", grant identifier 03XP0509B and "CatSE 2", grant identifier 03XP0510E.

Open access funding enabled and organized by Projekt DEAL.

Conflict of Interest

The authors declare no competing financial interests.

Data Availability Statement

The data that support the findings of this study are available from the corresponding author upon reasonable request.

Keywords

CCD, dendrites, Li-metal anode, short circuit, solid-state batteries

Received: July 24, 2023
Revised: September 29, 2023
Published online: October 19, 2023

[1] J. Janek, W. G. Zeier, *Nat. Energy* **2016**, *1*, 16141.
[2] S. Randau, D. A. Weber, O. Kötz, R. Koerver, P. Braun, A. Weber, E. Ivers-Tiffée, T. Adermann, J. Kulisch, W. G. Zeier, F. H. Richter, J. Janek, *Nat. Energy* **2020**, *5*, 259.
[3] W. D. Richards, L. J. Miara, Y. Wang, J. C. Kim, G. Ceder, *Chem. Mater.* **2016**, *28*, 266.
[4] M. Li, J. Lu, Z. Chen, K. Amine, *Adv. Mater.* **2018**, *30*, 1800561.
[5] J.-M. Tarascon, M. Armand, *Nature* **2001**, *414*, 359.
[6] T. Krauskopf, F. H. Richter, W. G. Zeier, J. Janek, *Chem. Rev.* **2020**, *120*, 7745.
[7] N. Nitta, F. Wu, J. T. Lee, G. Yushin, *Mater. Today* **2015**, *18*, 252.
[8] X. B. Cheng, R. Zhang, C. Z. Zhao, Q. Zhang, *Chem. Rev.* **2017**, *117*, 10403.
[9] T. Fuchs, J. Becker, C. G. Haslam, C. Lerch, J. Sakamoto, F. H. Richter, J. Janek, *Adv. Energy Mater.* **2023**, *13*, 2202712.
[10] S.-K. Otto, T. Fuchs, Y. Moryson, C. Lerch, B. Mogwitz, J. Sann, J. Janek, A. Henss, *ACS Appl. Energy Mater.* **2021**, *4*, 12798.
[11] S.-K. Otto, Y. Moryson, T. Krauskopf, K. Peppler, J. Sann, J. Janek, A. Henss, *Chem. Mater.* **2021**, *33*, 859.
[12] Y. Zhu, X. He, Y. Mo, *J. Mater. Chem. A* **2016**, *4*, 3253.
[13] Y. Zhu, J. G. Connell, S. Tepavcevic, P. Zapol, R. Garcia-Mendez, N. J. Taylor, J. Sakamoto, B. J. Ingram, L. A. Curtiss, J. W. Freeland, D. D. Fong, N. M. Markovic, *Adv. Energy Mater.* **2019**, *9*, 1803440.
[14] J. G. Connell, T. Fuchs, H. Hartmann, T. Krauskopf, Y. Zhu, J. Sann, R. Garcia-Mendez, J. Sakamoto, S. Tepavcevic, J. Janek, *Chem. Mater.* **2020**, *32*, 10207.
[15] S. Otto, L. M. Riegger, T. Fuchs, S. Kayser, P. Schweitzer, S. Burkhardt, A. Henss, J. Janek, *Adv. Mater. Interfaces* **2022**, *9*, 2102387.
[16] H. Schmalzried, J. Janek, *Ber. Bunsenges. Phys. Chem.* **1998**, *143*, 127.
[17] V. Raj, V. Venturi, V. R. Kankanallu, B. Kuiri, V. Viswanathan, N. P. B. Aetukuri, *Nat. Mater.* **2022**, *21*, 1050.
[18] H. Huo, Y. Chen, R. Li, N. Zhao, J. Luo, J. G. Pereira Da Silva, R. Mücke, P. Kaghazchi, X. Guo, X. Sun, *Energy Environ. Sci.* **2020**, *13*, 127.
[19] H. Huo, Y. Chen, N. Zhao, X. Lin, J. Luo, X. Yang, Y. Liu, X. Guo, X. Sun, *Nano Energy* **2019**, *61*, 119.
[20] A. Sharafi, E. Kazyak, A. L. Davis, S. Yu, T. Thompson, D. J. Siegel, N. P. Dasgupta, J. Sakamoto, *Chem. Mater.* **2017**, *29*, 7961.
[21] A. Sharafi, C. G. Haslam, R. D. Kerns, J. Wolfenstine, J. Sakamoto, *J. Mater. Chem. A* **2017**, *5*, 21491.
[22] C. Wang, Y. Gong, B. Liu, K. Fu, Y. Yao, E. Hitz, Y. Li, J. Dai, S. Xu, W. Luo, E. D. Wachsman, L. Hu, *Nano Lett.* **2017**, *17*, 565.
[23] G. T. Hitz, D. W. Mcowen, L. Zhang, Z. Ma, Z. Fu, Y. Wen, Y. Gong, J. Dai, T. R. Hamann, L. Hu, E. D. Wachsman, *Mater. Today* **2019**, *22*, 50.
[24] F. Flatscher, M. Philipp, S. Ganschow, H. M. R. Wilkening, D. Rettenwander, *J. Mater. Chem. A* **2020**, *8*, 15782.
[25] L. Porz, T. Swamy, B. W. Sheldon, D. Rettenwander, T. Frömling, H. L. Thaman, S. Berendts, R. Uecker, W. C. Carter, Y. Chiang, *Adv. Energy Mater.* **2017**, *7*, 1701003.
[26] T. Krauskopf, B. Mogwitz, H. Hartmann, D. K. Singh, W. G. Zeier, J. Janek, *Adv. Energy Mater.* **2020**, *10*, 2000945.
[27] G. Mcconohy, X. Xu, T. Cui, E. Barks, S. Wang, E. Kaeli, C. Melamed, X. W. Gu, W. C. Chueh, *Nat. Energy* **2023**, *8*, 423.
[28] F. Flatscher, M. Philipp, S. Ganschow, H. M. R. Wilkening, D. Rettenwander, *J. Mater. Chem. A* **2020**, *8*, 15782.
[29] J. Kasemchainan, S. Zekoll, D. Spencer Jolly, Z. Ning, G. O. Hartley, J. Marrow, P. G. Bruce, *Nat. Mater.* **2019**, *18*, 1105.
[30] T. Krauskopf, H. Hartmann, W. G. Zeier, J. Janek, *ACS Appl. Mater. Interfaces* **2019**, *11*, 14463.
[31] Y. Lu, C. Zhao, J. Hu, S. Sun, H. Yuan, Z. Fu, X. Chen, J.-Q. Huang, M. Ouyang, Q. Zhang, *Sci. Adv.* **2022**, *8*, eadd0510.
[32] T. Krauskopf, R. Dippel, H. Hartmann, K. Peppler, B. Mogwitz, F. H. Richter, W. G. Zeier, J. Janek, *Joule* **2019**, *3*, 2030.
[33] J. A. Lewis, C. Lee, Y. Liu, S. Y. Han, D. Prakash, E. J. Klein, H.-W. Lee, M. T. Mcdowell, *ACS Appl. Mater. Interfaces* **2022**, *14*, 4051.
[34] V. Reisecker, F. Flatscher, L. Porz, C. Fincher, J. Todt, I. Hanghofer, V. Hennige, M. Linares-Moreau, P. Falcaro, S. Ganschow, S. Wenner, Y.-M. Chiang, J. Keckes, J. Fleig, D. Rettenwander, *Nat. Commun.* **2023**, *14*, 2432.
[35] E. G. Herbert, W. E. Tenhaeff, N. J. Dudney, G. M. Pharr, *Thin Solid Films* **2011**, *520*, 413.
[36] W. S. Lepage, Y. Chen, E. Kazyak, K.-H. Chen, A. J. Sanchez, A. Poli, E. M. Arruda, M. D. Thouless, N. P. Dasgupta, *J. Electrochem. Soc.* **2019**, *166*, A89.
[37] Z. Ning, G. Li, D. L. R. Melvin, Y. Chen, J. Bu, D. Spencer-Jolly, J. Liu, B. Hu, X. Gao, J. Perera, C. Gong, S. D. Pu, S. Zhang, B. Liu, G. O. Hartley, A. J. Bodey, R. I. Todd, P. S. Grant, D. E. J. Armstrong, T. J. Marrow, C. W. Monroe, P. G. Bruce, *Nature* **2023**, *618*, 287.

[38] S.-Y. Ham, H. Yang, O. Nunez-Cuacuas, D. H. S. Tan, Y.-T. Chen, G. Deysher, A. Cronk, P. Ridley, J.-M. Doux, E. A. Wu, J. Jang, Y. S. Meng, *Energy Storage Mater.* **2023**, *55*, 455.
[39] C. D. Fincher, C. E. Athanasiou, C. Gilgenbach, M. Wang, B. W. Sheldon, W. C. Carter, Y.-M. Chiang, *Joule* **2022**, *6*, 2794.
[40] H. Buschmann, J. Dölle, S. Berendts, A. Kuhn, P. Bottke, M. Wilkening, P. Heitjans, A. Senyshyn, H. Ehrenberg, A. Lotnyk, V. Duppel, L. Kienle, J. Janek, *Phys. Chem. Chem. Phys.* **2011**, *13*, 19378.
[41] L. Cheng, W. Chen, M. Kunz, K. Persson, N. Tamura, G. Chen, M. Doeff, *ACS Appl. Mater. Interfaces* **2015**, *7*, 2073.
[42] N. J. Taylor, S. Stangeland-Molo, C. G. Haslam, A. Sharafi, T. Thompson, M. Wang, R. Garcia-Mendez, J. Sakamoto, *J. Power Sources* **2018**, *396*, 314.
[43] P. Albertus, S. Babinec, S. Litzelman, A. Newman, *Nat. Energy* **2018**, *3*, 16.
[44] M. J. Wang, E. Kazyak, N. P. Dasgupta, J. Sakamoto, *Joule* **2021**, *5*, 1371.
[45] J. K. Eckhardt, T. Fuchs, S. Burkhardt, P. J. Klar, J. Janek, C. Heiliger, *ACS Appl. Mater. Interfaces* **2022**, *14*, 42757.
[46] J. K. Eckhardt, P. J. Klar, J. Janek, C. Heiliger, *ACS Appl. Mater. Interfaces* **2022**, *14*, 35545.
[47] W. Zaman, L. Zhao, T. Martin, X. Zhang, Z. Wang, Q. J. Wang, S. Harris, K. B. Hatzell, *ACS Appl. Mater. Interfaces* **2023**, *15*, 37401.
[48] B. Kinzer, A. L. Davis, T. Krauskopf, H. Hartmann, W. S. LePage, E. Kazyak, J. Janek, N. P. Dasgupta, J. Sakamoto, *Matter* **2021**, *4*, 1947.
[49] D. K. Singh, T. Fuchs, C. Krempaszky, P. Schweitzer, C. Lerch, F. H. Richter, J. Janek, *Matter* **2023**, *6*, 1463.
[50] M. J. Wang, E. Carmona, A. Gupta, P. Albertus, J. Sakamoto, *Nat. Commun.* **2020**, *11*, 5201.
[51] C. Haslam, J. Sakamoto, *J. Electrochem. Soc.* **2023**, *170*, 040524.
[52] U. Wietelmann, M. Steinbild, *Lithium and Lithium Compounds. Ullmann's Encyclopedia of Industrial Chemistry*,**2014**, p. 1–38.
[53] T. Krauskopf, B. Mogwitz, C. Rosenbach, W. G. Zeier, J. Janek, *Adv. Energy Mater.* **2019**, *9*, 1902568.
[54] D. K. Singh, T. Fuchs, C. Krempaszky, B. Mogwitz, S. Burkhardt, F. H. Richter, J. Janek, *Adv. Funct. Mater.* **2023**, *33*, 2211067.
[55] K. Lee, E. Kazyak, M. J. Wang, N. P. Dasgupta, J. Sakamoto, *Joule* **2022**, *6*, 2547.
[56] C. G. Haslam, J. B. Wolfenstine, J. Sakamoto, *J. Power Sources* **2022**, *520*, 230831.
[57] M. J. Wang, R. Choudhury, J. Sakamoto, *Joule* **2019**, *3*, 2165.
[58] Z. Ning, D. S. Jolly, G. Li, R. De Meyere, S. D. Pu, Y. Chen, J. Kasemchainan, J. Ihli, C. Gong, B. Liu, D. L. R. Melvin, A. Bonnin, O. Magdysyuk, P. Adamson, G. O. Hartley, C. W. Monroe, T. J. Marrow, P. G. Bruce, *Nat. Mater.* **2021**, *20*, 1121.
[59] A. Sharafi, S. Yu, M. Naguib, M. Lee, C. Ma, H. M. Meyer, J. Nanda, M. Chi, D. J. Siegel, J. Sakamoto, *J. Mater. Chem. A* **2017**, *5*, 13475.
[60] B. Zhao, W. Ma, B. Li, X. Hu, S. Lu, X. Liu, Y. Jiang, J. Zhang, *Nano Energy* **2022**, *91*, 106643.
[61] M. Klimpel, H. Zhang, M. V. Kovalenko, K. V. Kravchyk, *Commun Chem* **2023**, *6*, 192.
[62] J. H. Cho, K. Kim, S. Chakravarthy, X. Xiao, J. L. M. Rupp, B. W. Sheldon, *Adv. Energy Mater.* **2022**, *12*, 2200369.
[63] T. Fuchs, C. G. Haslam, A. C. Moy, C. Lerch, T. Krauskopf, J. Sakamoto, F. H. Richter, J. Janek, *Adv. Energy Mater.* **2022**, *12*, 2201125.
[64] T. Fuchs, B. Mogwitz, S. Otto, S. Passerini, F. H. Richter, J. Janek, *Batter Supercaps* **2021**, *4*, 1145.
[65] D. Spencer Jolly, Z. Ning, J. E. Darnbrough, J. Kasemchainan, G. O. Hartley, P. Adamson, D. E. J. Armstrong, J. Marrow, P. G. Bruce, *ACS Appl. Mater. Interfaces* **2020**, *12*, 678.
[66] D. K. Singh, A. Henss, B. Mogwitz, A. Gautam, J. Horn, T. Krauskopf, S. Burkhardt, J. Sann, F. H. Richter, J. Janek, *Cell Rep Phys Sci* **2022**, *3*, 101043.
[67] M. Weiss, R. Ruess, J. Kasnatscheew, Y. Levartovsky, N. R. Levy, P. Minnmann, L. Stolz, T. Waldmann, M. Wohlfahrt-Mehrens, D. Aurbach, M. Winter, Y. Ein-Eli, J. Janek, *Adv. Energy Mater.* **2021**, *11*, 2101126.
[68] A. Sharafi, H. M. Meyer, J. Nanda, J. Wolfenstine, J. Sakamoto, *J. Power Sources* **2016**, *302*, 135.